PREPARATION AND CHARACTERIZATION OF MAGNETITE Fe₃O₄ NANOPARTICLES

Kyawt Kyawt[1,2], Khin Mar Cho[3], Myat Kyaw Thu[4]

Abstract

Magnetite Fe_3O_4 nanoparticles were prepared by a chemical co-precipitation method using $FeSO_4.7H_2O$ and $FeCl_3$ as precursors. The prepared Fe_3O_4 nanoparticles were characterized by X-ray Diffraction Analysis (XRD), Scanning Electron Microscopy (SEM), Raman Spectroscopy, Fourier Transform Infrared Spectroscopy (FT IR), Thermo gravimetric Differential Thermal Analysis (TG-DTA) and UV-Visible Spectroscopy. The XRD patterns showed the formation of the single phase for Fe_3O_4 nanoparticles. The crystallite size of Fe_3O_4 nanoparticles was 16.91 nm when calculated by Scherrer equation. Fe_3O_4 nanoparticles showed face-centered cubic structure with a = 8.4099 Å. The SEM image of Fe_3O_4 nanoparticles revealed the agglomeration of the particles. In Raman spectrum the dominant peaks were observed at 211, 274, 380, 472, 584 and 653 when using the laser 532 nm excitation source. FT IR spectral data indicated the characteristic Fe-O stretching vibration at 540 cm^{-1}. TG-DTA thermogram showed the thermal stability of Fe_3O_4 nanoparticles beyond 300 ℃. The wavelength of maximum absorption of Fe_3O_4 nanoparticles was observed at 322 nm.

Keywords: Fe_3O_4 nanoparticles, magnetite, co-precipitation method, face-centered cubic

Introduction

Nano is a prefix used in front of a macroscopic unit to change its value by orders of magnitude. Nano means one billionth, or 10^{-9}. Thus, one nanometer is one billionth of a meter (Balzani, 2005). Nanoparticles are tiny materials with their sizes range from 1 to 100 nm. They can be classified into different classes according to their properties, shapes or sizes. Fullerenes, metal nanoparticles, ceramic nanoparticles, and polymeric nanoparticles are examples of different classes. Nanoparticles possess unique physical and chemical properties due to their high surface area and volume ratio. Their reactivity, toughness and other properties also depend on their unique size, shape and structure. Nanoparticles have found widespread applications in water treatment, energy production and contaminant sensing. In addition, an increasing number of literatures also describe how novel nanoparticles can be used to address major environmental challenges (Perreault *et al*., 2015).

Metal elements are able to form different types of oxide compounds. They adopt a number of structural geometries with an electronic structure with metallic, semiconductor or insulator character such as optical, optoelectronic, magnetic, electrical, thermal, electrochemical, photo- electrochemical, mechanical, and catalytic properties (Vayssieres, 2004).The efficiency of the aforesaid properties of metal oxides largely varies with the reduction of particle size into nanoscale and which is either enhanced or completely novel properties compared to their bulk materials (Zhang, 2008). Iron oxide nanoparticles have been attracting much attention of researchers for its environmental benignity, multivalent oxidation states, abundant polymorphism, mutual polymorphous changes in nanophase, nontoxicity and low cost (Zhu *et al*., 2014). The magnetic properties in the photocatalytic system make photocatalysts very easy to be separated and recycled from wastewater after using an external magnet (Nikazar *et al*., 2014).

[1] PhD Candidate, Department of Chemistry, University of Yangon
[2] Lecturer, Department of Chemistry, Bago University
[3] Associate Professor, Department of Chemistry, University of Yangon
[4] Professor, Department of Chemistry, University of Yangon

In addition, super paramagnetic Fe_3O_4 nanoparticles possess a promising adsorption capacity for contaminants along with optimal magnetic properties, showing rapid separation of the adsorbent from solution via a magnetic field (Chen *et al.*, 2011). Among different phases of iron oxide, the magnetite (Fe_3O_4), the maghemite (γ-Fe_2O_3), and the hematite (α-Fe_2O_3) are probably the most common for fundamental study and also very important in technologically. Magnetite (Fe_3O_4) assumes inverse cubic spinel structure in which iron cation exists in two oxidation states of Fe^{2+} and Fe^{3+} and hence shows very interesting properties. Magnetic properties of magnetite nanoparticles have been widely studied because of their relevance to magnetic recording, biomedical applications and so on (Daou *et al.*, 2006). Co-precipitation is probably the simplest and most efficient synthetic route to obtain magnetic particles. In co-precipitation, a stoichiometric mixture of ferrous and ferric precursors in aqueous medium are used as an iron source, which under alkaline conditions yield super paramagnetic nanoparticles. The size distribution in co-precipitation is relatively broad because in the precipitation process, nucleation and particle growth are both present and in competition. Nevertheless, co-precipitation is most widely used because it has the potential for industrialization (Pereira *et al.*, 2012).

The aim of the present study is to prepare Fe_3O_4 nanoparticles by chemical co-precipitation method and to study its structural, morphological and thermal properties.

Materials and Methods

Preparation of Fe_3O_4 Nanoparticles

Magnetite iron (III) oxide nanoparticles were prepared by using the route of chemical co-precipitation. In brief, 50 mL of 0.02 M of aqueous iron (II) sulphate hexahydrate ($FeSO_4.7H_2O$) solution was mixed thoroughly with 50 mL of 0.04 M of aqueous iron (III) chloride ($FeCl_3$) solution and heated to 80 ℃ with a vigorous magnetic stirring. While stirring, ammonium hydroxide solution was added until pH 11. The dark blackish brown precipitate obtained was filtered and washed thoroughly with deionized water for several times and dried at 100 ℃ for 12 h.

Characterization of Fe_3O_4 Nanoparticles

X-ray diffraction pattern of Fe_3O_4 nanoparticles were recorded on XRD diffractometer (MultiFlex 2kW Type, Rigaku. D/max 220, Japan) at Universities' Research Center, Yangon. X-ray patterns were recorded with CuKα radiation (λ=1.54056 Å) at 40 kV and 50 mA and the diffraction angle ranged from 10˚ to 70˚ of 2θ. Crystallite size of Fe_3O_4 nanoparticles was calculated by Scherrer's equation. Surface morphology of the prepared sample was studied by scanning electron microscope (JSM-5610LV, JEOL, Japan) at Universities' Research Center, Yangon. Molecular structure of the prepared sample was studied by Raman Spectrometer (Lab RAM HR 800, HORIBA, Japan) at Universities' Research Center, Yangon. Raman analysis was carried out with a laser at 532 nm excitation source. Fourier transform infrared (FT IR) Spectrum of the sample was recorded on FT IR spectrometer (FT-IR 8400, SHIMADZU, Japan) at Universities of Yangon. FT IR analysis was carried out in a range of wavenumber from 4000 to 400 cm^{-1}. Thermogravimetric-Differential Analysis (TG-TDA) was performed at Universities' Research Center, Yangon. TG-TDA thermogram was obtained by using Al_2O_3 as reference. The measurement was carried out at a heating rate of 20.0 k J min^{-1} and scanned from 40 ℃ to 600 ℃ with a scanning rate of 20 ℃ min^{-1}, under nitrogen atmosphere of 20 psi. UV-Visible absorption spectrum of the sample was recorded in a range of 200 nm to 800 by UV- Visible (SHIMADZU UV-2600), Japan at Bago University.

Results and Discussion

XRD Analysis of Prepared Fe_3O_4 Nanoparticles

The characterization of the resulting Fe_3O_4 particles after heat treatment was performed by means of X-ray diffraction (XRD) for confirming the presence of nanoparticles and analyzing its structure. The XRD pattern of Fe_3O_4 nanoparticles is illustrated in Figure 1. Six diffraction peaks were observed at 2θ values of 30.099˚, 35.391˚, 43.248˚, 53.322˚, 56.909° and 62.540° corresponding to Miller indices (220), (311), (400), (422), (511), and (440), respectively and a single phase of Fe_3O_4 nanoparticles was observed (Table 1). These peaks were in well agreement with the standard Fe_3O_4 (72-2303 > Magnetite Fe_3O_4). Since the Miller indices were all odd and all even Fe_3O_4 nanoparticles were indexed as face-centered cubic with a = 8.4099 Å. The average crystallite size of Fe_3O_4 nanoparticles was 16.91 nm using Sherrer's equation (Table 2).
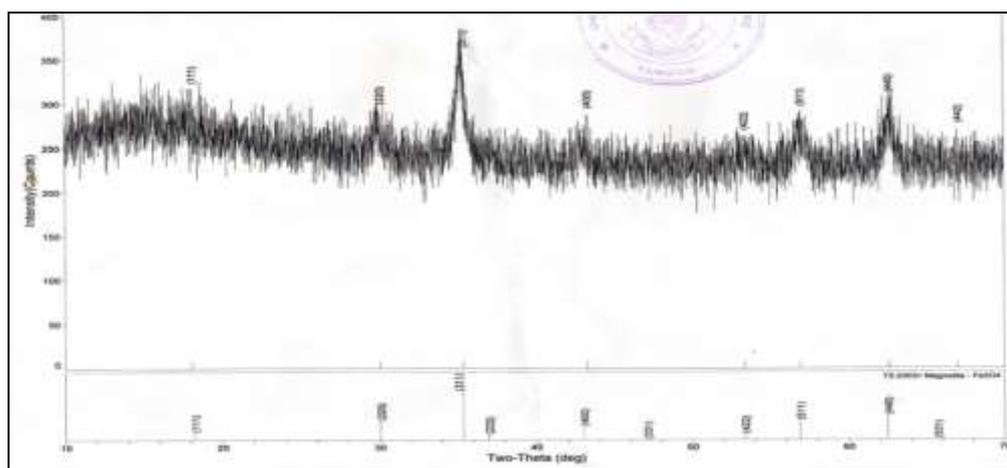
Figure 1 XRD diffractogram of Fe_3O_4 nanoparticles

Table 1 Phase Identification of Fe_3O_4 Nanoparticles

No.	Diffraction Angle '2θ' (°)	Interplanar Spacing 'd' (Å)	Miller Indices (hkl)	Phase ID
1	30.099	2.9665	220	Fe_3O_4
2	35.391	2.5341	311	Fe_3O_4
3	43.248	2.0902	400	Fe_3O_4
4	53.322	1.7167	422	Fe_3O_4
5	56.909	1.6167	511	Fe_3O_4
6	62.540	1.4840	440	Fe_3O_4

Table 2 Lattice Parameter, Crystal Structures and Average Crystallite Size of Fe_3O_4 nanoparticles

Sample	Lattice Parameters						Crystal Structures	Average Crystallite Size (nm)
	Axial Length (Å)			Interaxial Angle (°)				
	a	b	c	α	β	γ		
Fe_3O_4 nanoparticles	8.4099	8.4099	8.4099	90	90	90	Cubic	16.91

SEM Analysis of Prepared Fe₃O₄ Nanoparticles

The morphological study was done by using SEM. The SEM micrograph (Figure 2) shows the formation of large agglomerates of nanoscale particles. It can be attributed to the growth by coalescence of nuclei, resulting in particles that tend to aggregate.
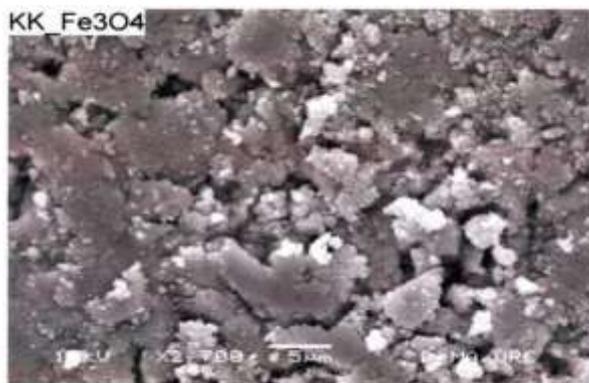
Figure 2 SEM micrograph of Fe_3O_4 nanoparticles

Raman Characterization

The Raman spectrum of Fe_3O_4 nanoparticles having six Raman active modes of (A_{1g} + $2E_g$ +$3T_{2g}$) is illustrated in Figure 3. The vibrational frequencies at 211 cm^{-1} ($T_{2g\,(1)}$), 274 cm^{-1} (E_g), 380cm^{-1} (E_g), 472 cm^{-1} ($T_{2g\,(2)}$), 584 cm^{-1} ($T_{2g\,(3)}$) and 653 cm^{-1} (A_{1g}), respectively, when using the laser 532 nm. A_{1g} band is due to the symmetric stretching of oxygen atoms ('breathing motion') in the tetrahedral FeO_4 group, along the (111) direction (Iliev *et al.*, 2011). Vibrational modes of E_g and $T_{2g(2)}$ were attributed to the symmetric and asymmetric bending of oxygen with respect to iron in the tetrahedral void respectively. The remaining two Raman modes were due to the motion of both oxygen and iron cations at the tetrahedral sites: the $T_{2g(3)}$ mode through an asymmetric stretching of iron and oxygen, and the $T_{2g(1)}$ mode through the complete translation of the FeO_4 unit within the spinel unit cell. Reported values in the literature for these vibrations are 193 ($T_{2g(1)}$), 306 (E_g), 450–490 ($T_{2g(2)}$), 538 ($T_{2g(3)}$)and 668 cm^{-1} (A_{1g}) for the magnetite case (Shebanova and Lazor, 2003).
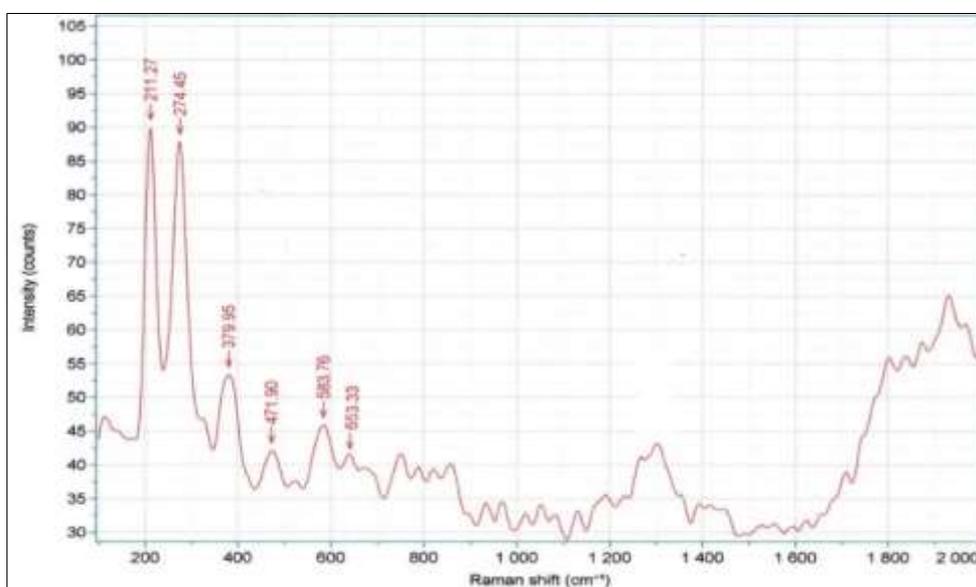
Figure 3 Raman spectrum of Fe_3O_4 nanoparticles

J. Myanmar Acad. Arts Sci. 2021 Vol. XIX. No.1A

427

Table 3 Raman Spectral Data Interpretation of Fe₃O₄ Nanoparticles

No.	Raman shift (cm⁻¹)			Peak Assignment
	Observed values	Reported values*		
1	211	193	$T_{2g(1)}$	translatory movement of the whole Fe_3O_4
2	274	306	E_g	symmetric bend of oxygen with respect to Fe
3	380	336	E_g	symmetric bend of oxygen with respect to Fe
4	472	450-490	$T_{2g(2)}$	asymmetric stretch of Fe and O
5	584	538	$T_{2g(3)}$	asymmetric bend of oxygen with respect to Fe
6	653	668	A_{1g}	symmetric stretch of oxygen atoms along Fe–O bonds

*Shebanova and Lazor , 2003

FT IR Analysis

The prepared Fe_3O_4 nanoparticles were analyzed by FTIR spectroscopy technique in order to find out the functional groups present in the particles. FT IR spectrum of Fe_3O_4 nanoparticles is shown in Figure 4 and the corresponding spectral data were presented in Table 4. From FT IR spectral data, the characteristic Fe-O stretching vibration was observed at 580 cm⁻¹. The abroad band at 3369 cm⁻¹ was due to O-H stretching vibration and O-H bending vibration was also observed at 1455 cm⁻¹.
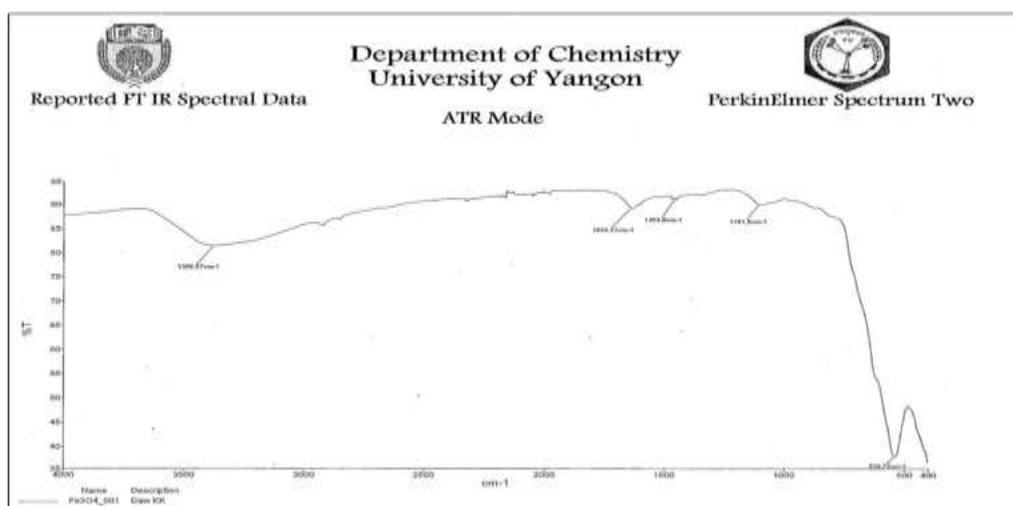
Figure 4 FT IR spectrum of Fe_3O_4 nanoparticles

Table 4 FT IR Spectral Data Interpretation of Fe₃O₄ Nanoparticles

No.	Wavenumber (cm⁻¹)		Band Assignment
	Observed values	Reported values	
1	3369	3000 - 3600*	O-H stretching vibration
2	1455	1200 - 1450*	O-H bending Vibration
3	580	577**	Fe-O stretching vibration

* Willard *et al.*, 1965
* * Farrokhi *et al.*, 2014

TG-DTA Analysis

TG-DTA is based on the changes in physical and chemical properties of material, when the temperature is increasing, measuring the difference in the weight and providing information about the composition and the purity of the sample. The sample is usually in the solid state and the changes that occur on heating include melting, phase transition, sublimation and decomposition. The decomposition temperature for the three different precursors was determined in order to know the influence of the precursor design on the structure and morphology of the obtained nanoparticles (Shriver, 2006).

TG-DTA analysis is performed for Fe_3O_4 nanoparticles between 40 °C to 600 °C. TG-DTA thermogram of Fe_3O_4 nanoparticles is shown in Figure 5 and the corresponding thermal data are presented in Table 5. From TG-DTA thermogram, two endothermic peaks were observed. Between the temperatures 30 °C to 120 °C the weight loss was about 7.07 % due to removal of adsorbed water molecules on the surface. Between 110 °C to 250 °C the weight loss was about 2.2 % due to removal of residual water molecules. Beyond 300 °C, Fe_3O_4 nanoparticles were thermally stable. The total weight loss for Fe_3O_4 nanoparticles was 11.05 %.
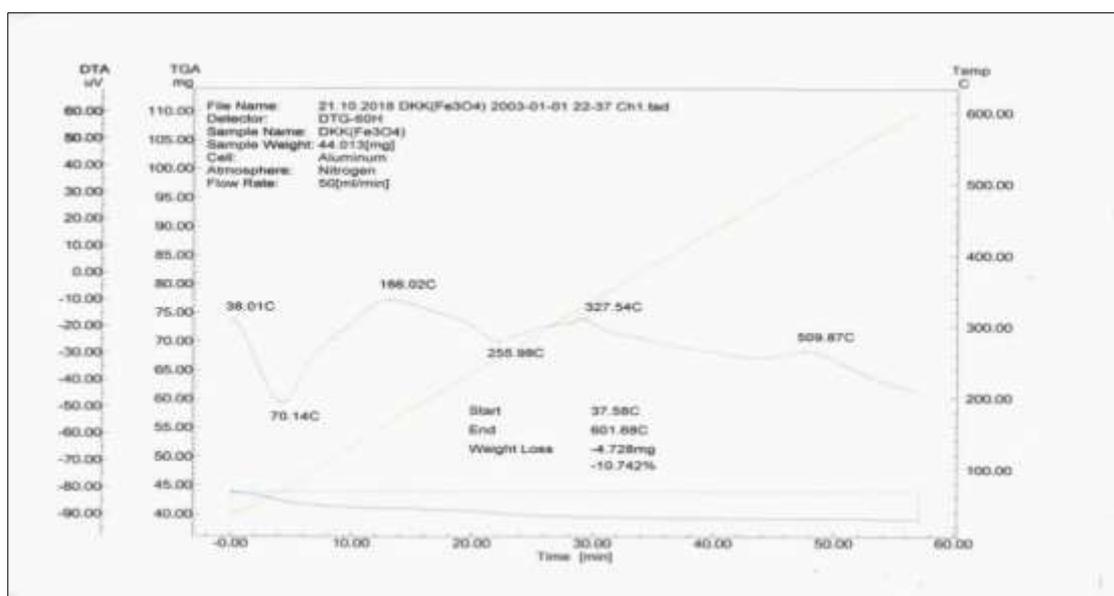
Figure 5 TG-DTA thermogram of Fe_3O_4 nanoparticles

Table 5 TG-DTA Data of Fe_3O_4 Nanoparticles

No.	Temperature Range (ºC)	Break in Temperature(ºC)	Weight loss (%)	Nature of peak	Remark
1	37.58 - 120	70.14	7.07	Endothermic peak	Removal of adsorbed water
2	120 - 310	255.98	2.2	Endothermic peak (very small)	Removal of residual water
3	310 - 601.68	-	1.78	-	Thermally stable

UV-Visible Spectroscopy

UV-Visible spectrophotometer was used to study the optical absorption. The optical absorption spectrum for Fe_3O_4 nanoparticles is shown in Figure 6. From UV-Visible absorption spectrum, it was observed that the maximum absorption peak of Fe_3O_4 nanoparticles was 322 nm. This could be due to the excitation of nanoparticles from ground state to excited state (Rajendran and Sengodan, 2017).
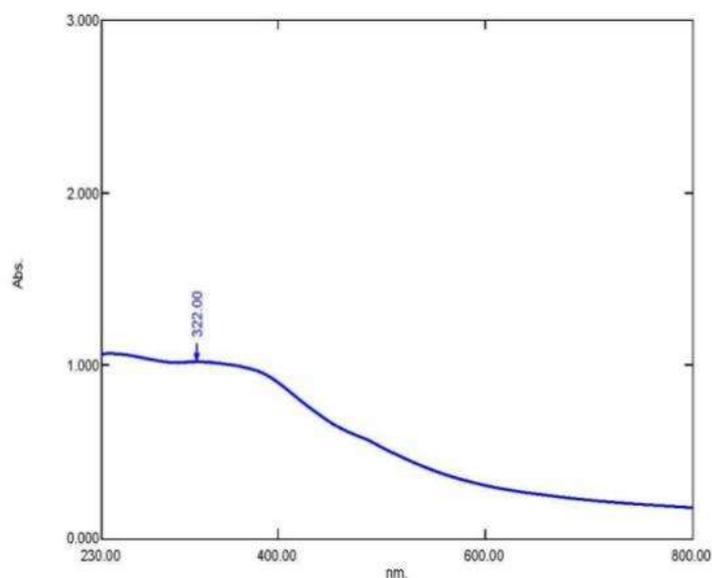
Figure 6 UV-Visible absorption spectrum of Fe_3O_4 nanoparticles

Conclusion

From the overall assessment of the present research work, the following inferences would be drawn. In this research, magnetic iron oxide (Fe_3O_4) nanoparticles was prepared by co-precipitation of Fe^{2+} and Fe^{3+} salts solution with ammonium hydroxide solution. Resulting sample was analyzed utilizing XRD, SEM, Raman spectroscopy, FT IR, TG-TDA, and UV-Visible methods. The Fe_3O_4 nanoparticles were indexed as cubic with a crystallite size of 16.91 nm. SEM image of Fe_3O_4 nanoparticles were generally spherical in shape and that they tend to form agglomerates and connect tightly to one another to form groups. From Raman spectroscopy, Fe_3O_4 nanoparticles had six Raman active modes including the characteristic peak of Fe_3O_4 at 653 cm^{-1}. It revealed the main phase of magnetite. From FT IR spectral data, Fe-O stretching vibration was observed at 580 cm^{-1}. TG-TDA analysis revealed the thermally stable of Fe_3O_4 nanoparticles beyond 300 °C. From UV-Visible absorption spectrum, the wavelength of maximum absorption of Fe_3O_4 nanoparticles was found at 322 nm. This result suggest that the Fe_3O_4 nanoparticles had strong light absorption properties in the ultraviolet and visible light range and can degrade organic pollutants in the wide spectral range.

Acknowledgements

References

Balzani, V. (2005). "Nanoscience and Nanotechnology: A Personal View of a Chemist". *Small*, vol. 1(3), pp.278-283

Chen, C., Gunawan, P. and Xu, R. (2011). "Self-Assembled Fe_3O_4-Layered Double Hydroxide ColloidalNanohybrids with Excellent Performance for Treatment of Organic Dyes in Water". *Journal of Materials Chemistry*, vol. 21, pp. 1218-1225

Daou, T., Pourroy, J., Be´gin-Colin, G., Grene`che, S., Ulhaq-Bouillet, J. M., Legare, C., Bernhardt, P., Leuvrey,P. and Rogez. G. (2006). "Hydrothermal Synthesis of Monodisperse Magnetite Nanoparticles". *Chem Mater.*, vol. 18, pp. 4399-4404

Farrokhi, M., Seyydeh-Cobra, H., Jae-Kyu, Y. and Shirzard-Siboni, M. (2014). "Application of Fe_3O_4–ZnO Nanocomposite on the Removal of Azo Dye from Aqueous Solution: Kinetics and Equilibrium Studies''.*J. Water Air Soil Pollute*, vol. 325 (211), pp.1-12

Iliev, M. N., Mazumdar, D., Ma, J. X., Gupta, A., Rigato, F. and Fontcuberta, J. (2011). "Monitoring B-site Ordering and Strain Relaxation in $NiFe_2O_4$ Epitaxial Films by Polarized Raman Spectroscopy". *Phys Rev. B,* vol. 83, pp. 014108

Nikazar, M., Alizadeh M., Lalavi R. and Rostami, M.H. (2014). " The Optimum Conditions for Synthesis of Fe_3O_4/ZnO Core/Shell Magnetic Nanoparticles for Photodegradation of Phenol". *Iranian J. Environ. Health Sci. Eng.*, vol. 12 (21), pp.3-6

Pereira, C., Pereira, A. M., Fernandes, C., Rocha, M., Mendes, R., Fernandez-Garcia, M. P., Guedes, A., Tavares, P. B., Greneche, J. M., jo, J. P. A. and Freire, C. (2012). "Superparamagnetic MFe_2O_4 (M = Fe, Co, Mn)

Nanoparticles: Tuning the Particle Size and Magnetic Properties through a Novel One-Step Coprecipitation Route". *Chem. Mater.*, vol. 24, pp.1496-1504

Perreault, F., de Faria, A. F. and Elimelech, M. (2015). "Environmental Applications of Graphene-Based

Nanomaterials". *Chem. Soc. Rev.,* pp. 390

Rajendran, S.P. and Sengodan, K. (2017). "Synthesis and Characterization of Zinc Oxide and Iron Oxide Nanoparticles Using Sesbania Grandiflora Leaf Extract as Reducing Agent". *Journal of Nanoscience* vol.2017, pp.1-11

Shebanova, O.N. and Lazor, P. (2003). "Raman Spectroscopic Study of Magnetite ($FeFe_2O_4$): A New

Assignment for the Vibrational Spectrum". *Journal of Solid State Chemistry,* vol.174, pp. 424-430

Shriver, D.F. and Atkins, P.W. (2006). *Inorganic Chemistry*. Oxford: 4^{th}Ed. Oxford University Press, pp.189-190

Vayssieres, L. (2004). "On the Design of Advanced Metal Oxide Nanomaterials," *Int. J. of Nanotechnology*, vol.1, pp. 1-40

Willard, H.H., Merritt, L.L. and Dean, J.A. (1965). *Instrumental Method of Analysi*. New York: 4th Edition, D.   Van Nostrand Co., Inc., pp. 142-143

Zhang, M. (2008). *Nonaqueous Synthesis of Metal Oxide Nanoparticles and Their Surface Coating*. Ph.D., University of New Orleans

Zhu, J., Simon Ng, K. Y. and Deng, D. (2014). "Micro Single Crystals of Hematite with Nearly 100% Exposed {104} Facets: Preferred Etching and Lithium Storage". *Cryst.Growth Des.*, vol. 14,